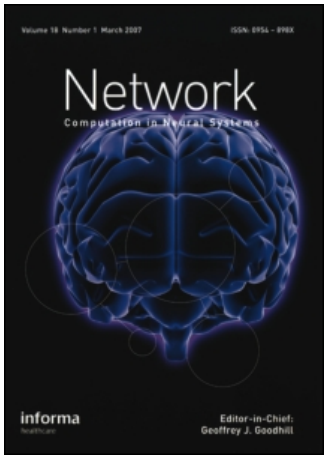

Network: Computation in Neural Systems
Publication details, including instructions for authors and subscription information:
http://www.informaworld.com/smpp/title~content=t713663148

A model for the thick, thin and pale stripe organization of primate V2

Nicholas V. Swindale [a]
[a] Department of Ophthalmology and Visual Sciences, University of British Columbia, Vancouver, B.C., Canada

First Published on: 24 September 2007
To cite this Article: Swindale, Nicholas V. (2007) 'A model for the thick, thin and pale stripe organization of primate V2', Network: Computation in Neural Systems, 18:4, 327 - 342
To link to this article: DOI: 10.1080/09548980701648472
URL: http://dx.doi.org/10.1080/09548980701648472

Network: Computation in Neural Systems
December 2007; 18(4): 327–342

informa
healthcare

A model for the thick, thin and pale stripe organization of primate V2

NICHOLAS V. SWINDALE

Department of Ophthalmology and Visual Sciences, University of British Columbia, 2550 Willow St., Vancouver, B.C., Canada V5Z 3N9

(Received 10 July 2007; accepted 27 August 2007)

Abstract
Models based on the idea of dimension reduction have been successful in describing the patterns of ocular dominance, spatial frequency and orientation preference found in primate V1. It is shown here that this approach can be extended to describe the organization of thick, thin and pale cytochrome oxidase stripes of primate V2 given an appropriately constructed stimulus space which includes a 3-valued variable which co-varies with color, orientation and disparity. The model successfully describes several aspects of V2 organization, including the fact that there are two pale stripes for each thick and thin stripe and the strong tendency for stripes to run perpendicular to the V1 border. In addition it predicts the presence of reversals in the direction of mapping of retinal eccentricity which should be more common in the pale stripes than elsewhere.

Keywords: *V2, self-organizing map, Kohonen, cytochrome oxidase, thin stripes, thick stripes, pale stripes*

Introduction

The combined maps of visual space, ocular dominance and orientation preference found in the primary visual cortex of higher mammalian species have been of interest to modelers for several decades. Despite the apparent structural complexity of these maps, very simple models, based on the concept of dimension reduction (Durbin and Mitchison 1990; Obermayer et al. 1990), have been successful in reproducing their morphological features (Erwin et al. 1995; Swindale 1996).

Correspondence: Nicholas V. Swindale, Department of Ophthalmology and Visual Sciences, University of British Columbia, 2550 Willow St., Vancouver, B.C., Canada V5Z 3N9. E-mail: swindale@interchange.ubc.ca

ISSN 0954-898X print/ISSN 1361-6536 online/07/040327–342 © 2007 Informa UK Ltd.
DOI: 10.1080/09548980701648472

These include the periodic branching stripe pattern of ocular dominance (Goodhill and Willshaw 1990), the continuous periodic representation of orientation with point singularities preferentially located in the centers of ocular dominance stripes or patches (Durbin and Mitchison 1990; Obermayer et al. 1990), and a tendency for orthogonal gradient relationships between pairs of patterns (Swindale 2000; Carreira-Perpiñán et al. 2005; Yu et al. 2005). The models proposed to account for these phenomena are based on the idea that the map patterns are the result of an attempt to map a multi-dimensional stimulus space onto a 2-dimensional (2D) surface (the cortex) subject to completeness and continuity constraints. Here, completeness means that all points in the space, or some appropriately chosen subset of them, should be represented in the map. Continuity means that nearby points in the 2D cortex should have similar stimulus values and that fractures or other discontinuities in the map should be minimized as far as possible, given the conflicting completeness constraint.

The formulation of a model in this framework has two stages: first, the construction of a multi-dimensional stimulus space within which stimuli are distributed in an appropriate way and second, given appropriately structured initial conditions, the application of a suitable method for generating a mapping of a 2D surface into this space that satisfies some combination of completeness and continuity constraints. The stimulus space (or manifold) that is typically used consists of a 2D sheet for the retina, points at the ends of a line for ocular dominance, and points on a circle for orientation. Additional dimensions may be added to account for other variables, such as spatial frequency (Yu et al. 2005) or direction preference (Swindale and Bauer 1998) that may also be represented in V1 maps. Two methods that have commonly been used to accomplish the mapping are the Elastic Net (Durbin and Willshaw 1987) and Kohonen Self Organizing Feature Map (Kohonen 1982) algorithms. Both algorithms produce patterns of ocular dominance and orientation columns that are visually very similar to those observed experimentally.

Compared to V1, the structure of primate V2 has seemed much less amenable to modeling. Anatomically, V2 consists of a strip of cortex about 3–6 mm wide which lies adjacent to the anterior border of V1 (Figure 1). Although narrow in width, the total area of V2 is comparable to that of V1 (Gattass et al. 1981). The posterior border with V1 represents the midline (vertical meridian) of the visual field while the anterior border represents the horizontal meridian. The visual field representation is thus split, with the upper half of V2 representing the lower visual field quadrant and vice versa. Cytochrome oxidase (CO) staining (Figure 1) reveals a pattern of alternating pale and dark bands, oriented perpendicular to the long axis of the area (Tootell and Silverman 1981; Livingstone and Hubel. 1982; Tootell et al. 1983). The dark bands themselves alternate in width and darkness, and are referred to as thin-dark and thick-dark stripes (or more commonly, just ''thin stripes'' and ''thick stripes''), respectively. Physiologically, the pale and thick stripes have been shown to contain orientation selective neurons (Hubel and Livingstone 1987; Malach et al. 1994; Vanduffel et al. 2002); the thin (dark) stripes contain predominantly non-oriented neurons selective for color (Hubel and Livingstone 1987; Tootell and Hamilton 1989; Moutoussis and Zeki 2002; Xiao et al. 2003; Lu and Roe 2007) while the thick stripes contain disparity selective cells (Roe and Ts'o 1995) with a bias towards vertical orientations (Ts'o et al. 2001). There is evidence for an

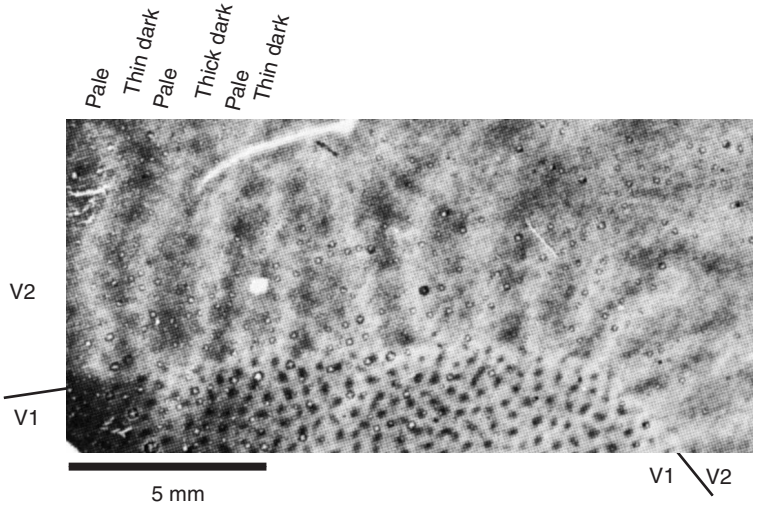

Figure 1. Cytochrome oxidase stain of a flat-mount section through the upper layers of squirrel monkey visual cortex showing an alternating sequence of pale, thin dark and thick dark stripes in V2 and an array of spots in V1. Anterior is upwards and dorsal is to the right. Differences between thick and thin stripes are subtle in this picture but are more apparent if viewed from a distance; thin stripes are also more darkly staining than the thick stripes (reproduced from Tootell et al. 1983). Pale stripes are believed to contain predominantly orientation selective neurons, thin dark stripes contain predominantly non-oriented neurons selective for color, while the thick stripes contain disparity selective cells. See text for further details.

ordered columnar representation of color in the thin stripes (Xiao et al. 2003; Tootell et al. 2004) and of disparity in the thick stripes (Ts'o et al. 2001).

Beyond the fact that they are present at birth, (Horton and Hocking 1996a) little is known about the development of V2 stripes or of factors that might influence the organization of the adult pattern. This, combined with the complexity of the thick-pale-thin-pale organization, might suggest that simple modeling of V2, in the spirit of the dimension-reduction approach to V1 that has been so successful, would not be possible. It is shown here that, to the contrary, the organization of at least some aspects of V2 can be modeled in a relatively simple way. Although the model arguably does not give insights into V2 function that go beyond those that already exist, it is possible that it might serve as a framework for a more principled approach in the future.

The model

Roe and Ts'o (1995) and Shipp and Zeki (2002) studied the representation of the visual field within V2. They confirmed earlier findings (Allman and Kaas 1974; Gattass et al. 1981) that the vertical meridian of the visual field is represented along the V1/V2 border. Lines of iso-polarity (i.e., meridians or lines of constant angle relative to the fovea) are mapped parallel to the border with the horizontal meridian

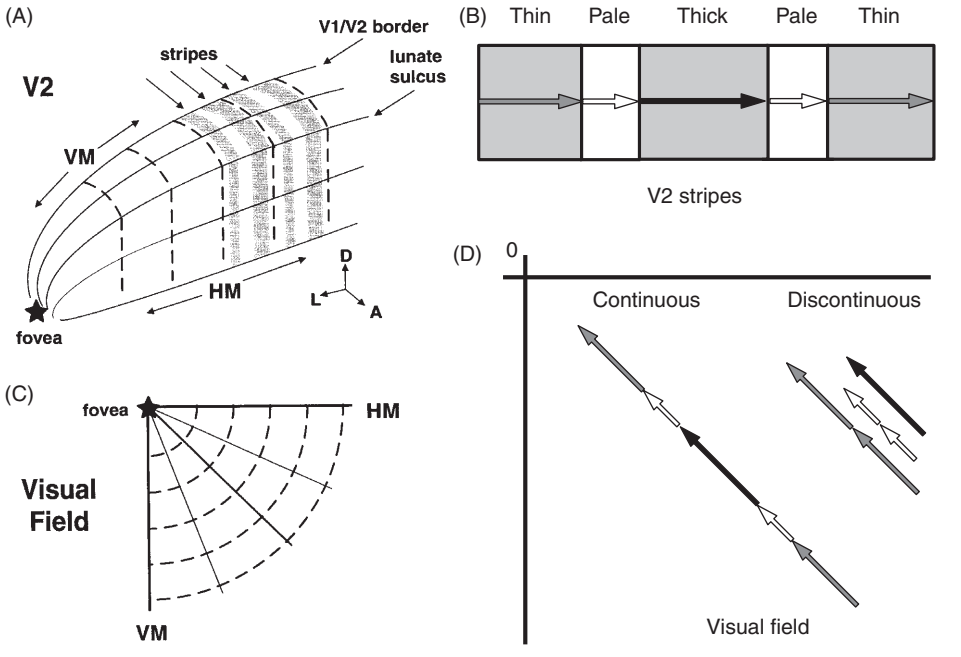

Figure 2. (A) Depiction of the retinotopic map in V2 in cortical co-ordinates, showing a region roughly comparable in size to that in Figure 1. Lines of constant meridional angle (solid lines in the visual field representation shown below, (C) run parallel to the V1/V2 border, and lines of constant visual field eccentricity (dashed) run perpendicular to the border, parallel to the thick and thin stripes. VM = vertical meridian; HM = horizontal meridian. (B) Possible mappings of visual field eccentricity across the thin, pale and thick stripes; (D) a *continuous* mapping, resulting in some visual field positions being unrepresented in particular kinds of stripe and a *discontinuous* mapping in which each visual field eccentricity is represented in each type of stripe. Note that the hypothesized direction of retinotopic mapping is the same in each stripe. (Redrawn from Roe and Ts'o 1995).

represented at the anterior edge of V2 (Figure 2A). Lines of constant eccentricity (distance from the fovea) are mapped perpendicular to the long axis of V2. This can be simply characterized as the projection of polar co-ordinates onto a rectilinear grid with lines of constant eccentricity running parallel to each other, intersecting lines of constant meridional angle at right angles. This means that the thick, thin and pale CO stripes run parallel to lines of constant eccentricity. It has been argued (Zeki and Shipp 1987; Roe and Ts'o 1995) that because different functional properties are represented in the different kinds of stripe, a continuous, smooth mapping of visual field position across the stripes is unlikely (Figure 2D). This is because certain properties (e.g., color) would only be represented at those visual field locations where the corresponding stripe (in this case thin dark) was represented. Instead they proposed, and presented evidence for, jumps and reversals in the retinotopic mapping at the border of each type of stripe such that each visual field location is represented in at least one thick, thin and pale stripe, ensuring uniform coverage of color (thin), depth (thick) and orientation (pale) across the visual field.

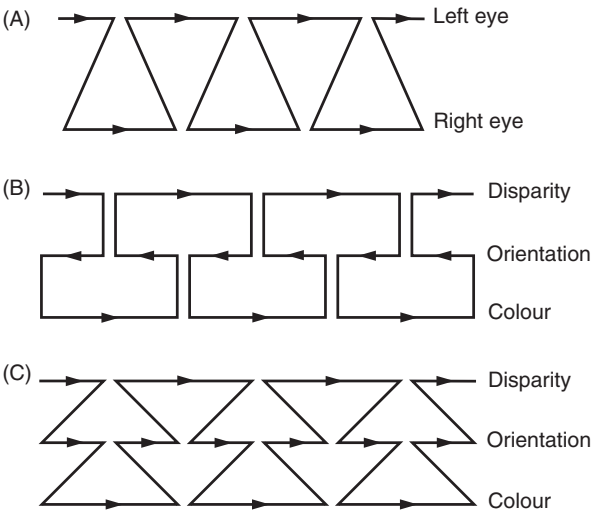

Figure 3. Types of retinotopic mapping into simple feature spaces. All three panels show projections of a 1D cortex into a 2D space where the horizontal axis is retinal position and the vertical axis represents either (A) the two values of ocular dominance or (B & C) the three values of color, orientation and disparity represented in V2 stripes.

The zigzagging of retinal representation at stripe borders is reminiscent of the jumps in receptive field position observed at the borders of ocular dominance columns (Hubel et al. 1974; Blasdel and Fitzpatrick 1984). These types of zig-zags, or foldings, are explained by dimension-reduction models as the result of the cortex attempting to map all positions in both eyes as continuously as possible. This is illustrated in Figure 3, which shows the simplified case of a mapping of a line (a 1-D cortex) into a 2D stimulus space where the horizontal axis is retinal position and the vertical axis is ocular dominance. Stimuli are chosen so that they lie on either of two horizontal, parallel lines in the space. Satisfaction of completeness and continuity constraints is obtained by mappings that minimize the total length of a line that joins all the possible stimuli. A locally optimal solution is a line that zigs back and forth, as shown in Figure 3A. Mappings obtained by the Kohonen or elastic net algorithms for the more realistic case where a 2D cortex must map to two parallel 2D sheets are more complex but show the same tendency for Z-shaped folds with jumps in retinotopic position correlating with jumps in ocular dominance.

The retinotopic distortions induced by the three types of stripes found in V2 (Roe and Ts'o 1995; Shipp and Zeki 2002) suggest that instead of mapping, like V1, a two-valued variable (eye type) plus a retina across its surface, V2 instead maps a three-valued variable. This variable co-varies with color, orientation and disparity. Since there is no known single stimulus feature (analogous to ocular dominance but with three discrete values) that co-varies with stripe type it must necessarily be regarded as fictitious, although of useful explanatory power. Figures 3B and 3C illustrate two possible ways in which such a mapping might be done, again for a simplified 1D cortex, in which the co-variable of orientation is assumed to lie between the positions of color and disparity. Note that this construction immediately explains why there are twice as many pale stripes as thick or

thin stripes. The first arrangement (Figure 3B), which is the more continuous of the two, avoids jumps in retinotopy where properties change, but the direction of retinotopy reverses locally in the orientation (pale) stripes. The second arrangement (Figure 3C) is less continuous because the total path length is longer and there are jumps in receptive field position, however the direction of retinotopy (as in the construction of Roe and Ts'o 1995) is the same in all types of stripe. This might be an important constraint, since the global organization of retinotopy in cortical maps is controlled by intrinsic factors (e.g., gradients of molecules) that are not taken directly into account by the simple types of model being considered here. Such gradients might well predetermine or bias the local directions of retinotopy in the maps.

Mathematical implementation

The Kohonen algorithm (Kohonen 1982) was used to model the development of V2 maps based on the preceding construction. The implementation of the algorithm was similar to that used previously (Swindale 2000, 2004). The stimulus vector was defined by $\mathbf{v} = \{x, y, a, u, v, \eta, l, m, s\}$ where (x, y) specify a visual field location within a rectangular region according to the transformation $x = \alpha \log_e r$, $y = \beta\phi$, where r and ϕ give eccentricity and meridional angular position in visual space in degrees, respectively and α and β are scaling constants (justification for this transformation is given below); a is the fictitious mapping variable; (u, v) are the components of stimulus orientation, θ, given by $u = R\cos(2\theta)$ and $v = R\sin(2\theta)$; η is disparity and (l, m, s) define the position of the stimulus in a 3D color/luminance space.

Cortical receptive fields were likewise given by the vector $\mathbf{w}_{i,j} = \{x, y, a, u, v, \eta, l, m, s\}$ where $\{x, y, a, \ldots\}$ are the receptive field values mapped to point (i, j) in the cortex.

The transformation of retinotopic position $x = \alpha \log_e r$, $y = \beta\phi$, maps points in a pie-shaped segment of visual space (i.e., between two meridia, and between two fixed eccentricities) onto a rectangular region, with a logarithmic scaling of eccentricity along the region's x-axis. This transformation was used for the following reasons. To begin with, the approximately 17×5 mm region of V2 being modeled (see below) represents nearly an entire visual field quadrant (Figure 2) within which there are large variations in magnification factor. It would be inappropriate to ignore these and assume locally uniform magnification as is often done in models of V1. Analysis of the description of ganglion cell densities in the macaque retina given by Azzopardi and Cowey (1996) shows that ganglion cell spacing scales nearly linearly with visual field eccentricity. This means that if their positions are projected according to the transformation, they will have an approximately uniform density over the space of x and y. Thus pairs of stimuli that are equal distances apart in the space of x and y are roughly equal distances apart measured in terms of ganglion cell numbers, which seems an appropriate metric to impose on the stimuli. Finally, if x is mapped linearly along the horizontal (i), cortical axis so that $x_i = i$, the transformation $x = \alpha \log_e r$ yields a cortical magnification factor $\mathrm{d}x/\mathrm{d}r = \alpha r^{-1}$ mm/deg which corresponds well to the value measured experimentally in V2 by Gattass et al. (1981) of $4r^{-1.1}$ mm/deg.

Following the presentation of a stimulus, cortical receptive fields change by an amount

$$\Delta \mathbf{w}_{i,j} = \varepsilon h(d)\left(\mathbf{v} - \mathbf{w}_{i,j}\right) \tag{1}$$

where ε is a rate constant, d is the distance in the cortex between the point whose receptive field is closest to $\mathbf{v}$ and point (i, j). $h(d)$ is a neighborhood function given by

$$h(d) = \exp\left(-\frac{d^2}{2\kappa^2}\right) \tag{2}$$

where κ is a width parameter.

Stimuli

Stimulus values were chosen according to the following set of rules: retinal position values (x, y) were chosen at random from a uniform distribution over the intervals $[\delta, X+\delta]$ and $[0, Y]$ where δ is a positive offset used to avoid the implication of an infinite stimulus density at $r=0$. Typically, $X=Y=12$. The mapping variable, a, took on values of -1, 0 or 1 with probabilities $p(1)=p_1$; $p(0)=p_2$; $p(-1)=p_3$. These values determine the widths of the three types of stripe. Normally $p_1=0.4$, $p_2=0.3$ and $p_3=0.3$. The value of a was used to constrain the values of the color, orientation and disparity components of the stimulus, as follows:

Color. $a=-1$; orientation $(u, v)=0$; disparity $(\eta)=0$; points (l, m, s) were chosen from a uniform distribution within a cube with sides of $D_c=2$ with the origin at zero (=black).

Orientation. $a=0$; orientations were uniformly randomly distributed on a circle with radius $R_\theta=1$; disparity $(\eta)=0$; color$(l, m, s)=0.5$.

Disparity. $a=1$; orientation angles had a Gaussian distribution with a mean $=90^\circ$ (vertical) and a standard deviation $\sigma_\theta=30^\circ$ and lay on a circle with radius $=0.5R_\theta$; disparity (η) had a Gaussian random distribution with $\sigma_\eta=1$; color $(l, m, s)=0.5$. The biased orientation distribution was chosen because of the likelihood that vertical orientations play a greater role in stereopsis than horizontal ones plus the evidence (Ts'o et al. 2001) that orientation preferences in thick stripes are clustered around vertical; the choice however has relatively little impact on the overall behavior of the model.

Figure 4 illustrates the construction of the stimulus space.

Initial cortical values

The cortex was $N \times M$ units in size with typically $N=200$ and $M=60$ corresponding to a region of V2 roughly 17×5 mm at a nominal scaling of 12 pixels/mm. A roughly ordered retinal topography was assumed to be present

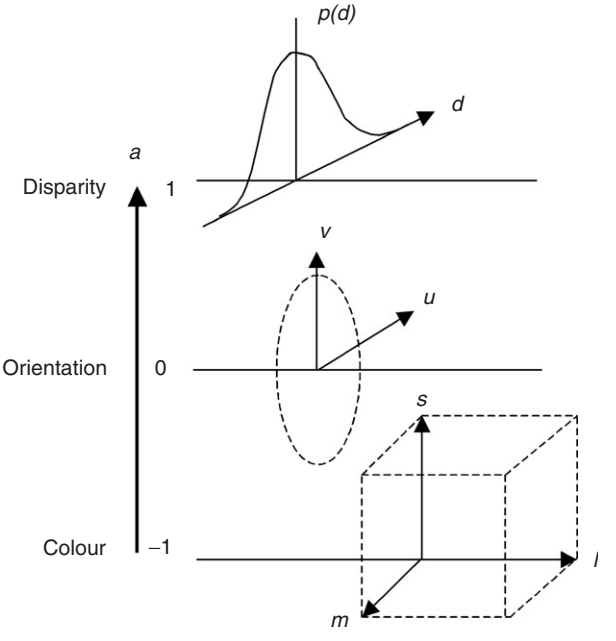

Figure 4. The construction of the stimulus space used to model V2.

initially, with cortical values of $x_{i,j} = iX/(N-1) + \xi_x$ and $y_{i,j} = jY/(M-1) + \xi_y$ where ξ_x and ξ_y were random numbers drawn from a Gaussian distribution with a mean of zero and a standard deviation $= \sigma_r$. Typically, $\sigma_r = 0.1$. Orientation values (u, v) were initially randomly distributed with means of zero and standard deviations $\sigma_\theta = 0.1$. Values of the mapping variable a, and disparity η, were likewise randomly distributed with means of zero and standard deviation $\sigma_a = \sigma_\eta = 0.1$. Color values l, m and s were randomly distributed around means of $D_c/2$ with $\sigma_c = 0.1$.

Simulations

The learning rate $\varepsilon = 0.01$. The following simulated annealing schedule was used: the neighborhood width, $\kappa = 6$ for the first 10^5 stimulus presentations, and was then reduced in size by multiplying by 0.99 every 5×10^3 stimuli. When it reached a lower limit of 1.0, at a total of about 10^6 stimulus presentations, it was kept constant and the simulation terminated after 2.5×10^6 stimulus presentations.

Periodic boundary conditions were used for the long axis of the cortex (the i-direction) and retina but not the narrow (j) axis, since this is intended to model the complete width of V2.

Results

A "cytochrome oxidase stain" of the model map was produced by plotting the magnitude of the cortical feature vector, $|\mathbf{v}|$, with dark regions representing large

values of the magnitude (Figures 5B and F). The overall magnitude is strongly influenced by the value of the fictitious mapping variable, a, which by design is small for regions where orientation is represented and large in the regions where color and disparity are represented. The ''stain'' nevertheless reproduces features seen in real CO stains of V2 not built in to the model, including the mottled appearance of the thick and thin stripes as well as the crenellated borders and light spots (which in the

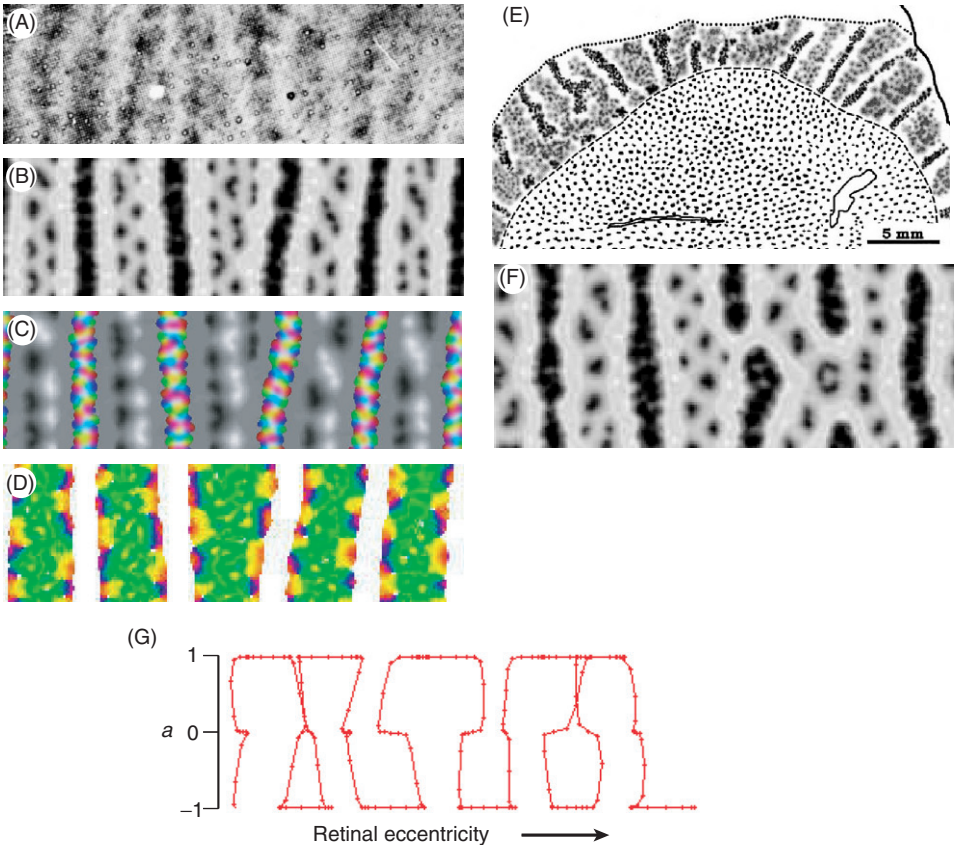

Figure 5. Model results. (A) A portion of the CO stain of V2 (Figure 1) shown for comparison; (B) results of a simulation in which the modulus of the cortical feature vector, $|\mathbf{v}|$, is plotted; white represents low values of the modulus, dark regions represent large values; (C) a combined representation of the values of disparity (η) shown in greyscale, and of color (l, m, s), from the simulation shown in (B); (D) the distribution of orientation angle in the same map; (orientation preference is absent in the thin stripes by construction). In (C) and (D) the value of the mapping variable, a, was used to partition the model cortex into regions defined as thick, thin and pale stripes. (E) A sketch of the CO staining pattern observed in a squirrel monkey showing regions where adjacent thick stripes fuse and obliterate thin stripes (taken from Figure 6B in Horton and Hocking, 1996b); (F) similar behavior observed in the model; (G) shows the projection of a single horizontal row of cortical points from the simulation shown in (B) into (a, x) space: each small red dot is a cortical pixel whose vertical position is given by its value of a, and whose horizontal position is given by its retinal eccentricity coordinate x. This can be compared with the ideal arrangement shown in Figure 3B.

model correspond to orientation singularities) within the pale stripes. Although there are no spatial asymmetries in the model apart from the elongated shape of the cortex, stripes show a strong preference for running perpendicular to the long axis of the cortex. Differences in the widths of the three kinds of stripe are largely determined by the values of p_1, p_2 and p_3.

Figure 5C shows, in a combined representation, the distribution of disparity and color preferences: dark and light blobs in the thick stripes represent the distribution of near and far disparity values while the mapping of color in the thin stripes is plotted by mapping the values of l, m and s to the red, green and blue values in the image. As is observed experimentally (Xiao et al. 2003; Lu and Roe 2007) particular colors have a patchy distribution within the thin stripes with nearby locations in the map representing similar colors.

Figure 5D shows the overall representation of orientation in the map with vertical orientations (green) represented in the thick stripes and a more uniform distribution of orientation preferences present at the borders, in the pale stripes. Singularities in the orientation map in the pale stripes appear as white dots in Figure 5B and correspond with low values of the feature vector modulus.

Real V2 stripes are not always perfectly regular and sometimes thin stripes are interrupted by the fusion of two adjacent thick stripes. Figure 5E shows examples of this, taken from Horton and Hocking (1996b). This behavior was reproduced in the model by relaxing the conditions that tend to produce stripes orthogonal to the long axis of the cortex. Figure 5F shows the results of a simulation where the size of the modeled region was changed from 200×60 pixels to 200×80 pixels, and slightly more disordered initial conditions ($\sigma_r = \sigma_a = \sigma_\eta = \sigma_c = 0.5$) were used.

The maps of retinal eccentricity produced by the model (Figure 5G) were generally more similar to the continuous prediction of Figure 3B, where the direction of retinotopy reverses in the pale stripes, than to the discontinuous but direction-preserving arrangement of Figure 3C. However, deviations from the ideal arrangement of Figure 3B were common, especially in simulations where the annealing was more rapid, or where initial conditions were more random than those used for Figure 5. In particular, positions where the direction of retinotopy reversed did not always coincide with pale stripe borders and were often located within the borders of the thick or thin stripes (Figure 6A). The direction of retinotopic mapping in the pale stripes was not always reversed and mappings could be flat (no magnification) and occasionally non-reversed. Local variations in magnification factor, including reversals, occurred within all three types of stripe (Figure 6A).

To quantify the extent to which reversals in the direction of mapping of retinal eccentricity were confined to the pale stripes, the percentage of retinotopically reversed pairs of points, i.e. for which $x_{i+1,j} < x_{i,j}$, was calculated for each type of stripe. Stripe type was defined as thin if $a < 0.5$, thick if $a > 0.5$ and pale otherwise. Table I shows that about a third of all pairs are reversed in the thick and thin stripes, and about two-thirds of all pairs are reversed in the pale stripes, for the simulation parameters used to obtain Figure 5B. Table I also shows the comparable values derived by visual inspection of the experimental data shown in Figures 6B and 6C. While the experimental data do not clearly show an increased presence of reversals in pale stripes, the interpretation is complicated by several difficulties: the

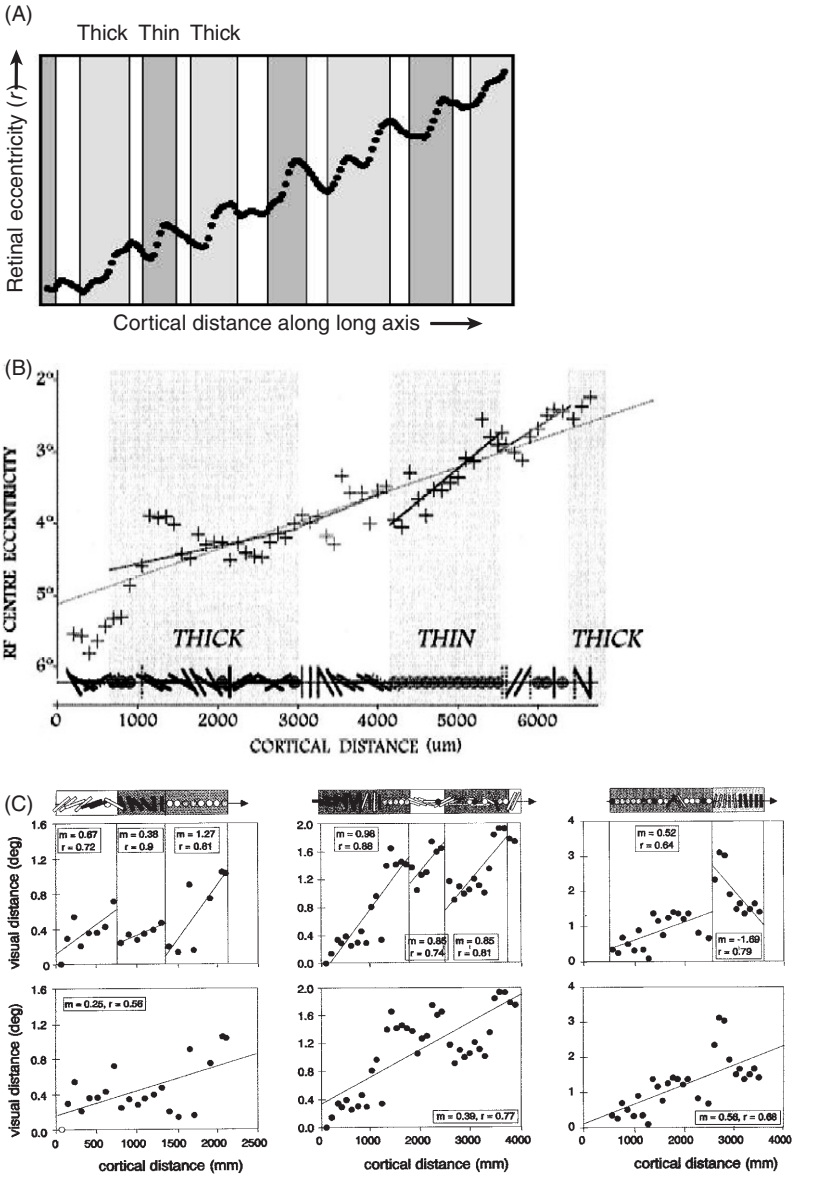

Figure 6. The mapping of visual field eccentricity across V2: (A) as produced by the model (same simulation as shown in 5B); (B) as reported by Shipp and Zeki (2002) and (C) by Roe and Ts'o (1995) in macaque monkey V2.

paucity of data (only 16 points in Figure 6C fall in pale stripes); the difficulty of aligning electrode positions with stripe borders determined by subsequent cytochrome oxidase staining, and the difficulty of measuring receptive field positions accurately in anesthetized animals. A similar comment on the same data is made by Sincich and Horton (2005).

Table I. The percentage of neighboring pairs of cortical points for which the direction of mapping of retinal eccentricity is reversed.

	Simulation (%)	Shipp and Zeki, 2002 (%)	Roe and Ts'o, 1995 (%)
Thin	32	43	44
Pale	63	48	20
Thick	29	38	38

Values are shown for the model (average of 3 different maps with different random initial conditions and identical parameters to the simulation shown in Figure 5B) and for the data of Shipp and Zeki (2002) and Roe and Ts'o (1995) shown in Figures 6B and 6C.

Discussion

Although the model appears to describe much of the organization of V2 as seen by CO staining quite successfully, much of this behavior is built in. In particular, the co-variation of color and disparity vectors with the mapping variable a, and the biasing of the model to produce stripes of unequal width (obtained by choosing appropriate values of p_1. p_2 and p_3) is what results in color being mapped to thin stripes, orientation to pale stripes and disparity to thick stripes. Thus the model does not give any direct insights into the reasons for those aspects of the organization of V2. The view of V2 organization and physiology that is reflected in the design of the stimulus space (Figure 4), is also very simple and is intended to highlight only the most basic and probable aspects of V2 architecture. In reality there are many uncertainties about what properties might, or might not, be represented in maps in V2 (see Sincich and Horton 2005 for a recent critical review). To begin with, many V2 neurons have receptive fields that perform more complex tasks than simply signaling values of color, orientation or disparity. For example, V2 neurons may signal information about relative rather than absolute disparities (Thomas et al. 2002); complex shapes (Hegde and Van Essen 2000; Ito and Komatsu 2004), subjective contours (Peterhans and von der Heydt 1993), motion defined borders (Marcar et al. 2000) and border ownership (Zhou et al. 2000). Whether any of these properties is mapped systematically is not yet known. However, the possibility that many of them might result from simply combining pairs of signals from V1 in an appropriate way (Ito and Komatsu 2004; Bredfeldt and Cumming 2006; Plebe 2007) might provide a basis for the construction of a more elaborate model of a V1–V2 mapping in the same spirit as those models that describe the mapping from retina to V1.

A further complication for the present model is that the parcellation of properties that are believed to be mapped within thin, pale and thick stripes may not be strict, but reflects instead a statistical tendency (Roe and Ts'o 1995; Felleman et al. 2005). Reinterpreting the model's output in a statistical sense would not be difficult (e.g. the magnitude of a cortical feature vector could be related to a population average), however it is puzzling that V2 maps should be relatively disorderly compared with V1 maps, where ordering (at least in cats) appears to be very precise (Ohki et al. 2005). Making the model more complex by incorporating additional and more complex attributes to the feature space, or making smaller changes such as allowing color and orientation to coexist would be possible and would probably not change the overall behavior of the model significantly.

An aspect of V2 organization that the model can claim to give insight into is the fact that there are two pale stripes for each thick or thin dark stripe. This is explained by the construction of Figure 3 and is based on the idea that there is an additional fictitious mapping variable that co-varies with color, orientation and disparity (or whatever other properties might be represented in the three types of stripe). The ordering of color, orientation and disparity along this axis suggests there is a sense in which color and orientation, and orientation and disparity, are more closely related pairs than are color and disparity. Superficially, this seems correct: color plays a limited role in disparity judgments (Simmons and Kingdom 1997) although some disparity selective neurons in V2 can show color selectivity (Roe and Ts'o 1995). Disparity and orientation cues seem likely to be closely linked, and most, if not all, disparity-tuned neurons are probably orientation selective. Likewise, color and orientation seem functionally linked, and many, though not all, color tuned neurons in V2 are orientation selective (Roe and Ts'o 1995). However, beyond these ideas there is no objective basis for choosing to represent the properties of orientation, color and disparity along an axis of some kind in the way that is done here. More generally, there is at present no principled answer to the question of why some properties might be combined in maps in the multidimensional tuning curves of individual neurons and others instead represented separately in nearby compartments within an area, as in V2, or represented far apart in different areas and processing streams (as for color and motion). Nor is it clear why some properties, such as direction preference, are represented in an orderly way in some primate cortical areas (e.g. MT, but not in others (e.g. V1). Formulation of a principled approach to these problems would be of enormous value in understanding the organization of the early visual pathways, but seems far off at present.

A second aspect of V2 organization that the model seems to explain in a natural way is the rather rigid parallel organization of stripes perpendicular to the V1/V2 border (notwithstanding the occasional branching thick stripe). This is the result of an anisotropic mapping of the retina (in this case of r and θ values projected into an iso-ganglion cell density representation in a square-shaped region) into an elongated cortical region. This behavior has previously been described and analyzed (Bauer 1995; Goodhill et al. 1997; Yu et al. 2005) in the case of ocular dominance stripes where the retina and cortex have different shapes. The effect may be related to a general tendency for pattern-forming mechanisms to produce stripes oriented perpendicular to the long axis of a pattern-forming region, when the wavelength of the stripes becomes comparable to the width of the region (Murray 1989) – as in the stripes on animal tails. In the present case however, elongation of the cortical region is not itself the main factor, as if the retinal mapping is made isotropic by making the dimensions of the retina (X and Y) congruent with the shape of the cortex the resulting stripe directions appear random and unrelated to the direction of elongation of the cortex. Also, elongated stripes form in a square cortical region, provided the input is from a rectangular retinal region (results not shown). Thus, it is the compression of the retinotopic map along one axis (the Y or ϕ axis) that causes stripes to run in a single direction.

The model also makes predictions about the kinds of retinotopic mappings that should be seen in the direction perpendicular to the stripes. Rather than discontinuous jumps, the model predicts that the mapping of eccentricity should be continuous, with the direction of retinotopy more often reversed in the pale

stripes than in the thick and thin stripes (Table I). In addition, the positions of reversals in the direction of retinotopy will not always be localized to stripe borders. The experimental findings of Shipp and Zeki (2002) provide modest support for this prediction (Figure 6B) since they show more or less continuous progressions of retinal eccentricity values across stripes, reversals in retinotopic direction that are not consistently aligned with stripe borders and a slight preponderance of reversals in pale stripes (Table I). The findings of Roe and Ts'o (1995) do not appear to fit the model (Figure 6C and Table I) although they can possibly be reconciled with it. The upper 3 panels of Figure 6C suggest, on the basis of linear regressions to the data in different functional sub-compartments (mostly, but not always in this study aligned with CO stripe borders), that sudden backward jumps are common and these allow the direction of retinotopy to remain the same (as in the construction of Figure 3C). An exception to this is the panel on the right of Figure 6C, which shows a forward jump followed by a reversal in direction, which is not predicted by either of the arrangements in Figure 3. However, the jumps are much less obvious if the data are viewed without superimposed regression lines (bottom 3 panels of Figure 3C). From this perspective, the data seem consistent with a degree of randomness in receptive field location (possibly real or reflecting measurement errors) accompanied by local variations in magnification factor and occasional reversals in the direction of mapping (right 2 panels of Figure 3C) similar to that reported by Shipp and Zeki (2002).

Acknowledgments

This work was supported by grants from the Natural Sciences and Engineering Research Council of Canada and the Canadian Institutes of Health Research.

References

Allman JM, Kaas JH. 1974. The organization of the second visual area (V-II) in the owl monkey: A second order transformation of the visual hemifield. Brain Res 76:247–265.

Azzopardi P, Cowey A. 1996. Models of ganglion cell topography in the retina of macaque monkeys and their application to sensory cortical scaling. Neuroscience 72:617–625.

Bauer H-U. 1995. Development of oriented ocular dominance bands as a consequence of areal geometry. Neural Comput 7:36–50.

Blasdel GG, Fitzpatrick D. 1984. Physiological organization of layer 4 in macaque striate cortex. J Neurosci 4:880–895.

Bredfeldt CE, Cumming BG. 2006. A simple account of cyclopean edge responses in macaque V2. J Neurosci 26:7581–7596.

Carreira-Perpiñán MA, Lister RJ, Goodhill GJ. 2005. A computational model for the development of multiple maps in primary visual cortex. Cereb Cortex 15:1222–1233.

Durbin R, Willshaw DJ. 1987. An analogue approach to the travelling salesman problem using an elastic net method. Nature 326:698–691.

Durbin R, Mitchison G. 1990. A dimension reduction framework for understanding cortical maps. Nature 343:644–647.

Erwin E, Obermayer K, Schulten K. 1995. Models of orientation and ocular dominance columns in the visual cortex: A critical comparison. Neural Comput 7:425–468.

Felleman DJ, Wang Y, Gutnisky DA. 2005. The spatial distribution of neuronal properties determines the functional organization of optical maps in macaque V2 thin stripes. Society for Neuroscience Abstracts 582.10.

Gattass R, Gross CG, Sandell JH. 1981. Visual topography of V2 in the macaque. J comp Neurol 201:519–539.

Goodhill GJ, Willshaw DJ. 1990. Application of the elastic net algorithm to the formation of ocular dominance stripes. Network 1:41–59.

Goodhill GJ, Bates KR, Montague PR. 1997. Influences on the global structure of cortical maps. Proc Roy Soc, Ser B 264:649–655.

Hegde J, Van Essen DC. 2000. Selectivity for complex shapes in primate visual area V2. J Neurosci 20:61–66.

Horton JC, Hocking DR. 1996a. An adult-like pattern of ocular dominance columns in striate cortex of newborn monkeys prior to visual experience. J Neurosci 16:1791–1807.

Horton JC, Hocking DR. 1996b. Anatomical demonstration of ocular dominance columns in striate cortex of the squirrel monkey. J Neurosci 16:5510–5522.

Hubel DH, Livingstone MS. 1987. Segregation of form, color, and stereopsis in primate area 18. J Neurosci 7:3378–3415.

Hubel DH, Wiesel TN, LeVay S. 1974. Visual field of representation in layer IVc of monkey striate cortex. Society for Neuroscience Abstracts 4th Annual Meeting, p. 264.

Ito M, Komatsu H. 2004. Representation of angles embedded within contour stimuli in area V2 of macaque monkeys. J.Neurosci 24:3313–3324.

Kohonen T. 1982. Self-organized formation of topologically correct feature maps. Biol Cybern 43:59–69.

Livingstone MS, Hubel DH. 1982. Thalamic inputs to cytochrome oxidase-rich regions in monkey visual cortex. Proc Natl Acad Sci USA 79:6098–6101.

Livingstone MS, Hubel DH. 1987. Psychophysical evidence for separate channels for the perception of form, color, movement, and depth. J Neurosci 7:3416–3468.

Lu HD, Roe AW. 2007 Functional organization of color domains in V1 and V2 of macaque monkey revealed by optical imaging. Cereb Cortex, advance online publication, June 18.

Malach R, Tootell RBH, Malonek D. 1994. Relationship between orientation domains, cytochrome oxidase stripes, and intrinsic horizontal connections in squirrel monkey area V2. Cereb Cortex 4:151–165.

Marcar VL, Raiguel SE, Xiao D, Orban GA. 2000. Processing of kinetically defined boundaries in areas V1 and V2 of the macaque monkey. J Neurophysiol 84:2786–2798.

Moutoussis K, Zeki S. 2002. Responses of spectrally selective cells in macaque area V2 to wavelengths and colors. J Neurophysiol 87:2104–2112.

Murray JD. 1989. Mathematical biology. Berlin-Heidelberg-New York: Springer.

Obermayer K, Ritter H, Schulten K. 1990. A principle for the formation of the spatial structure of cortical feature maps. Proc Natl Acad Sci USA 87:8345–8349.

Ohki K, Chung S, Ch'ng YH, Kara P, Reid RC. 2005. Functional imaging with cellular resolution reveals precise micro-architecture in visual cortex. Nature 433:597–603.

Peterhans E, von der Heydt R. 1993. Functional organization of area V2 in the alert macaque. Eur J Neurosci 5:509–524.

Plebe A. 2007. A model of angle selectivity development in visual area V2. Neurocomputing 70:2060–2063.

Roe AW, Ts'o DY. 1995. Visual topography in primate V2: Multiple representation across functional stripes. J Neurosci 15:3689–3715.

Shipp S, Zeki S. 2002. The functional organization of area V2, II: The impact of stripes on visual topography. Visual Neurosci 19:211–231.

Simmons DR, Kingdom FAA. 1997. On the independence of chromatic and achromatic stereopsis mechanisms. Vision Res 37:1271–1280.

Sincich LC, Horton JC. 2005. The circuitry of V1 and V2: Integration of color, form and motion. Annu Rev Neurosci 28:303–326.

Swindale NV. 1996. The development of topography in the visual cortex: A review of models. Network 7:161–247.

Swindale NV. 2000. How many maps are there in visual cortex? Cereb Cortex 10:633–643.

Swindale NV. 2004. How different feature spaces may be represented in cortical maps. Network 15:217–242.

Swindale NV, Bauer H-U. 1998. Application of Kohonen's self-organizing feature map algorithm to cortical maps of orientation and direction preference. Proc Roy Soc Lond Ser B 265:827–838.

Thomas OM, Cumming BG, Parker AJ. 2002. A specialization for relative disparity in V2. Nat Neurosci 5:472–478.

Tootell RB, Hamilton SL. 1989. Functional anatomy of the second visual area (V2) in the macaque. J Neurosci 9:2620–2644.

Tootell RBH, Silverman MS. 1981. A comparison of cytochrome oxidase and deoxyglucose patterns in macaque visual cortex. Soc Neurosci Abstracts 7:118.

Tootell RBH, Silverman MS, De Valois RL, Jacobs GH. 1983. Functional organization of the second cortical visual area in primates. Science 220:737–739.

Tootell RBH, Nelissen K, Vanduffel W, Orban GA. 2004. Search for color 'center(s)' in macaque visual cortex. Cereb Cortex 14:353–363.

Ts'o DY, Roe AW, Gilbert CD. 2001. A hierarchy of the functional organization for color, form and disparity in primate visual area V2. Vision Res 41:1333–1349.

Vanduffel W, Tootell RBH, Schoups AA, Orban GA. 2002. The organization of orientation selectivity throughout macaque visual cortex. Cereb Cortex 12:647–662.

Wolf F, Bauer H-U, Pawelzik K, Geisel T. 1996. Organization of the visual cortex. Nature 382:306–307.

Xiao Y, Wang I, Felleman DJ. 2003. A spatially organized representation of colour in macaque cortical area V2. Nature 421:535–539.

Yu H, Farley BJ, Jin DZ, Sur M. 2005. The coordinated mapping of visual space and response features in visual cortex. Neuron 47:267–280.

Zeki S, Shipp S. 1987. Functional segregation within area V2 of macaque money visual cortex. Seeing contour and color. Oxford: Pergamon Press. pp 120–124.

Zhou H, Friedman HS, von der Heydt R. 2000. Coding of border ownership in monkey visual cortex. J Neurosci 20:6594–6611.